Supporting Information

Molecular Bixbyite-Like In_{12}-Oxo Clusters with Tunable Functionalization Sites for Lithography Patterning Applications

Xiaofeng Yi[1], Di Wang[1,2], Fan Li[1,2], Jian Zhang[1] and Lei Zhang[1]*

[1]State Key Laboratory of Structural Chemistry, Fujian Institute of Research on the Structure of Matter, Chinese Academy of Sciences, Fuzhou, Fujian 350002, P. R. China.

[2] University of Chinese Academy of Sciences, Beijing 100049, P. R. China.

Email: LZhang@fjirsm.ac.cn

Content

I. General methods and materials

All the reagents and solvents employed are purchased commercially and used as received without further treatment. Propylene glycol 1-monomethyl ether 2-acetate (PGMEA), *p*-fluorophenol and $InBr_3$ were purchased from energy chemical. *p*-nitrophenol and $InCl_3 \cdot 4H_2O$ were purchased from Aladdin. While isopropanol (IPA), methanol, phenol, tetrahydrofuran and diethanolamine were bought from Sino pharm Chemical Reagent Beijing. Powder X-ray diffraction (PXRD) analyses data were mounted on a Rigaku Mini Flex II diffractometer using Cu Kα radiation (λ = 1.54056 Å) under ambient conditions. The Fourier transform infrared (FT-IR) spectra (KBr pellets) were performed on Brucker VERTEX 70 over a range of 400-4000 cm^{-1}. Thermal stabilities were investigated by a Mettler Toledo TGA/SDTA 851e analyzer in N_2 atmosphere with a heating rate of 10 °C/min under N_2 atmosphere. The electrospray ionization mass spectrometry (ESI-MS) data were collected on Impact II UHR-TOF (Bruker). Elemental analyses were measured on a Vario MICRO Elemental Analyzer instrument. The UV−vis absorption spectra are recorded at room temperature on a Lamda35 UV spectrophotometer and scanned at 268-800 nm. The energy dispersive spectroscopy (EDS) analyses of single crystals were performed on a JEOL JSM6700F field-emission scanning electron microscope equipped with an Oxford INCA system. The film thickness was measured by Ellipsometry-J. A. Woollam V-VASE. The film was exposed to an electron-beam using Raith quantum. The topography and the surface roughness of the sample are characterized by means of AFM-Brucker Dimension ICON and Asylum Research-Cypher. SEM images for patterns are performed by Zeiss Supra55.

II. Synthesis

Synthesis of **InOC-1**: A mixture of $InCl_3 \cdot 4H_2O$ (293 mg, 1 mmol), diethanolamine (1 mL), CH_3OH (3 mL) was sealed in a 20 mL vial and transferred to an oven at 100 °C for 2 days. When cooled to room temperature, block colorless crystals formed. (yield: 210 mg, 95.56% based on In). Elemental analysis (%) for $C_{36}H_{86}Cl_6In_{12}N_8O_{26}$, *calc.*: C, 16.39; H, 3.29; N, 4.25; found: C, 16.36; H, 3.46; N, 4.23.

Synthesis of **InOC-2**: A mixture of $InBr_3 \cdot 4H_2O$ (354 mg, 1 mmol), diethanolamine (1.5 mL), CH_3OH (3 mL) was sealed in a 20 mL vial and transferred to an oven at 100 °C for 2 days. When cooled to room temperature, block colorless crystals formed. (yield: 155mg, 61.99% based on In). Elemental analysis (%) for $C_{39}H_{98}Br_6In_{12}N_8O_{29}$, *calc.*: C, 15.61; H, 3.29; N, 3.73; found: C, 15.87; H, 3.27; N, 3.87.

Synthesis of **InOC-3**: A mixture of $InCl_3 \cdot 4H_2O$ (293 mg, 1 mmol), *p*-nitrophenol (700 mg, 5 mmol), diethanolamine (1 mL), tetrahydrofuran (4 mL) was sealed in a 20 mL vial and transferred to an oven at 100 °C for 2 days. When cooled to room temperature, block yellowish crystals formed. The crystals are washing with tetrahydrofuran before collected. (yield: 120mg, 46.97% based on In). Elemental analysis (%) for $C_{56}H_{90}Cl_6In_{12}N_{12}O_{34}$, *calc.*: C, 21.94; H, 2.96; N, 5.48; found: C, 22.16; H, 2.84; N, 5.40.

Synthesis of **InOC-4**: A mixture of $InBr_3 \cdot 4H_2O$ (354 mg, 1 mmol), *p*-nitrophenol (700 mg, 5 mmol), diethanolamine (0.5 mL), tetrahydrofuran (4 mL) was sealed in a 20 mL vial and transferred to a oven at 100 °C for 2 days. When cooled to room temperature, block yellowish crystals formed. (yield: 171mg, 61.58% based on In). Elemental analysis (%) for $C_{56}H_{90}Br_6In_{12}N_{12}O_{34}$, *calc.*: C, 20.18; H, 2.72; N, 5.04; found: C, 18.59; H, 3.02; N, 4.82.

Synthesis of **InOC-5**: A mixture of $InCl_3 \cdot 4H_2O$ (293 mg, 1 mmol), *p*-fluorophenol (550 mg, 5 mmol), diethanolamine (1 mL), tetrahydrofuran (4 mL) was sealed in a 20 mL vial and transferred to a oven at 100 °C for 2 days. When cooled to room temperature, block light crystals formed. (yield: 115mg, 46.67% based on In). Elemental analysis (%) for $C_{56}H_{90}Cl_6F_4In_{12}N_8O_{26} \cdot 2NH(CH_2CH_2OH)_2$, *calc.*: C, 24.26; H, 3.56; N, 4.42; found: C, 25.31; H, 3.44; N, 4.21.

III. Single-crystal X-ray diffraction

Single-crystal diffraction data for **InOC-1** and **InOC-2** were collected on Hybrid Pixel Array detector equipped with Ga-Kαradiation (λ= 1.3405 Å) at about 293~298 K, while **InOC-3**, **InOC-4** and **KLD-5** were collected on Supernova single crystal diffractometer equipped with graphite-monochromatic Cu-Kαradiation (λ= 1.54184Å) at about 100 K. Using Olex2,[1] the structures were solved with the dual-direct methods using ShelxT and refined with the full-matrix least-squares technique based on F^2 using the *SHELXL*.[2] Non-hydrogen atoms were refined anisotropically. Hydrogen atoms were added theoretically. The obtained crystallographic data for **InOC-1** to **InOC-5** summarized in Table S1 to Table S5. The X-ray crystallographic coordinates for structures reported in this article have been deposited at the Cambridge Crystallographic Data Centre (CCDC) under deposition numbers CCDC 2078614-2078618 (**InOC-1** to **InOC-5**). These data can be obtained free of charge from the Cambridge Crystallographic Data Centre via http://www.ccdc.cam.ac.uk/data_request/cif.

Table S1 Crystal data and structure refinement for **InOC-1**.

Crystal formula	$C_{36}H_{84}Cl_6In_{12}N_8O_{26}$
Formula weight	2635.65
Temperature/K	293(2)
Crystal system	monoclinic
Space group	I2
a/Å	16.05120(10)
b/Å	11.42060(10)
c/Å	20.21170(10)
α/°	90
β/°	90.1940(10)
γ/°	90
Volume/Å^3	3705.07(4)
Z	2
ρ_{calc}g/cm^3	2.362
μ/mm^{-1}	21.288
F(000)	2508.0
Crystal size/mm^3	0.8 × 0.7 × 0.6
Radiation	GaKα (λ = 1.3405)
Index ranges	$-21 \le h \le 20$, $-15 \le k \le 14$, $-27 \le l \le 27$
Reflections collected	43834

Independent reflections	9088 [R_{int} = 0.0720, R_{sigma} = 0.0361]
Data/restraints/parameters	9088/1/400
Goodness-of-fit on F^2	1.036
Final R indexes [I>=2σ (I)]	R_1 = 0.0335, wR_2 = 0.0911
Final R indexes [all data]	R_1 = 0.0340, wR_2 = 0.0915
Largest diff. peak/hole / e $Å^{-3}$	1.13/-1.33

Table S2 Crystal data and structure refinement for **InOC-2**.

Crystal formula	$C_{36}H_{84}Br_6In_{12}N_8O_{26}$
Formula weight	2902.41
Temperature/K	293(2)
Crystal system	triclinic
Space group	P-1
a/Å	11.5427(3)
b/Å	26.8196(3)
c/Å	26.8568(5)
α/°	101.1820(10)
β/°	102.181(2)
γ/°	96.092(2)
Volume/$Å^3$	7878.3(3)
Z	4
$\rho_{calc}g/cm^3$	2.447
μ/mm^{-1}	21.535
F(000)	5448.0
Crystal size/mm^3	0.1 × 0.08 × 0.06
Radiation	GaKα (λ = 1.3405)
Index ranges	$-14 \le h \le 14$, $-34 \le k \le 34$, $-28 \le l \le 34$
Reflections collected	104803
Independent reflections	34943 [R_{int} = 0.0750, R_{sigma} = 0.0721]
Data/restraints/parameters	34943/14/1602
Goodness-of-fit on F^2	1.045
Final R indexes [I>=2σ (I)]	R_1 = 0.0754, wR_2 = 0.1826

Final R indexes [all data]	R_1 = 0.1138, wR_2 = 0.2024
Largest diff. peak/hole / e Å^{-3}	2.39/-1.93

Table S3 Crystal data and structure refinement for **InOC-3**.

Crystal formula	$C_{56}H_{88}Cl_6In_{12}N_{12}O_{34}$
Formula weight	3063.92
Temperature/K	100.0(2)
Crystal system	tetragonal
Space group	I-4
a/Å	15.9892(2)
b/Å	15.9892(2)
c/Å	20.3659(5)
α/°	90
β/°	90
γ/°	90
Volume/Å^3	5206.63(18)
Z	2
ρ_{calc}g/cm^3	1.954
μ/mm^{-1}	22.853
F(000)	2940.0
Crystal size/mm^3	0.11 × 0.1 × 0.05
Radiation	CuKα (λ = 1.54184)
Index ranges	-15 ≤ h ≤ 19, -16 ≤ k ≤ 19, -25 ≤ l ≤ 24
Reflections collected	19375
Independent reflections	5146 [R_{int} = 0.0559, R_{sigma} = 0.0410]
Data/restraints/parameters	5146/61/276
Goodness-of-fit on F^2	1.048
Final R indexes [I>=2σ (I)]	R_1 = 0.0565, wR_2 = 0.1445
Final R indexes [all data]	R_1 = 0.0601, wR_2 = 0.1484
Largest diff. peak/hole / e Å^{-3}	1.23/-1.40

Table S4 Crystal data and structure refinement for **InOC-4**.

Crystal formula	$C_{56}H_{68}Br_6In_{12}N_{12}O_{34}$
Formula weight	3310.52
Temperature/K	100.01(12)
Crystal system	tetragonal
Space group	I-4
a/Å	16.1018(4)
b/Å	16.1018(4)
c/Å	20.4257(8)
α/°	90
β/°	90
γ/°	90
Volume/Å^3	5295.7(3)
Z	2
ρ_{calc}g/cm^3	2.076
μ/mm^{-1}	23.728
F(000)	3116.0
Crystal size/mm^3	0.12 × 0.1 × 0.06
Radiation	CuKα (λ = 1.54184)
Index ranges	$-11 \le h \le 19$, $-19 \le k \le 16$, $-24 \le l \le 17$
Reflections collected	7312
Independent reflections	4325 [R_{int} = 0.0407, R_{sigma} = 0.0464]
Data/restraints/parameters	4325/156/276
Goodness-of-fit on F^2	1.067
Final R indexes [I>=2σ (I)]	R_1 = 0.0759, wR_2 = 0.1999
Final R indexes [all data]	R_1 = 0.0793, wR_2 = 0.2069
Largest diff. peak/hole / e Å^{-3}	1.71/-2.14

Table S5 Crystal data and structure refinement for **InOC-5**.

Crystal formula	$C_{56}H_{88}Cl_6F_4In_{12}N_8O_{26}$
Formula weight	2955.88
Temperature/K	100.03(19)
Crystal system	tetragonal
Space group	I-4
a/Å	15.9744(2)
b/Å	15.9744(2)
c/Å	19.4804(5)
α/°	90
β/°	90
γ/°	90
Volume/Å^3	4971.04(18)
Z	2
ρ_{calc}g/cm^3	1.975
μ/mm^{-1}	23.891
F(000)	2828.0
Crystal size/mm^3	0.08 × 0.06 × 0.05
Radiation	CuKα (λ = 1.54178)
Index ranges	$-17 \leq h \leq 17$, $-17 \leq k \leq 16$, $-21 \leq l \leq 21$
Reflections collected	10192
Independent reflections	3465 [R_{int} = 0.0303, R_{sigma} = 0.0257]
Data/restraints/parameters	3465/36/254
Goodness-of-fit on F^2	1.086
Final R indexes [I>=2σ (I)]	R_1 = 0.0275, wR_2 = 0.0709
Final R indexes [all data]	R_1 = 0.0280, wR_2 = 0.0712
Largest diff. peak/hole / e Å^{-3}	1.48/-0.58

IV. Bond valence sum calculations

Bond valence sum calculations[3] are performed on **InOC-1** (**Table S6**), **InOC-2** (**Table S7**), **InOC-3** (**Table S8**), **InOC-4** (**Table S9**) and **InOC-5** (**Table S10**). The BVS values for the oxygen atoms suggest that there exists protonation of some oxygen positions in the skeleton of these In_{12}-oxo-clusters with BVS value of *ca.* 1.

Table S6 Bond valence sum values for oxygen atoms in **InOC-1**.

O00J	–1.98	O1	–1.98	O2	–1.95	O3	–1.91	O4	–2.04
O5	**–1.05**	O6	–1.97	O7	–2.07	O8	–1.96	O9	–1.93
O10	–2.01	**O11**	**–1.01**	O12	–2.05	O13	–1.96		

Table S7 Bond valence sum values for oxygen atoms in **InOC-2**.

O1	–1.95	O2	–1.96	O3	–1.94	**O4**	**–1.00**	O5	–1.83
O6	–1.95	O7	–2.01	O8	–2.06	O9	–1.95	O10	–1.90
O11	–1.99	O12	–2.10	O13	–1.80	O14	–1.98	O15	–2.03
O16	–2.05	O17	–1.94	O18	–2.03	O19	–2.03	O20	–1.92
O21	–2.01	**O22**	**–1.02**	O23	–2.00	O24	–2.02	O25	–2.04
O26	–1.94	O27	–1.93	O28	–2.03	**O29**	**–1.03**	O30	–2.06
O31	–1.97	O32	–2.08	O33	–1.94	O34	–1.98	O35	–1.99
O36	–2.06	O37	–2.10	O38	–1.87	O39	–2.00	O40	–1.98
O41	–2.05	O42	–1.89	O43	–2.03	O44	–1.73	O45	–1.95
O46	–1.83	O47	–2.05	O48	–2.02	O49	–2.03	O50	–1.96
O51	**–1.06**	O52	–2.01						

Table S8 Bond valence sum values for oxygen atoms in **InOC-3**.

O3	–2.43	O4	–2.03	O5	–2.05	**O6**	**–1.08**	O7	–2.17
O8	–1.89	O9	–2.04						

Table S9 Bond valence sum values for oxygen atoms in **InOC-4**.

O3	–2.11	O4	–2.26	**O5**	**–1.08**	O6	–2.04	O7	–1.91
O8	–2.08	O9	–1.88						

Table S10 Bond valence sum values for oxygen atoms in **InOC-5**.

O1	–2.00	**O2**	**–1.07**	O3	–2.19	O4	–2.03	O5	–2.02
O6	–1.87	O7	–2.03						

V. Additional structural pictures

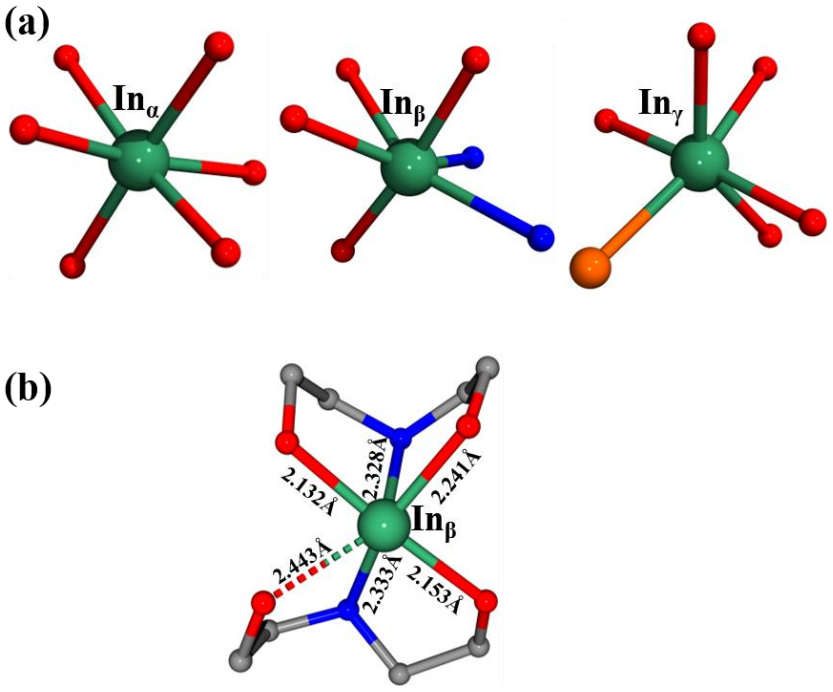

Figure S1 (a) The coordination environment of In_α $\{InO_6\}$, In_β $\{InO_5Cl\}$ and In_γ $\{InO_4N_2\}$ in **InOC-1** to **InOC-5**. **(b)** Structural details and coordination modes of diethanol amine in **InOC-1** to **InOC-5**.

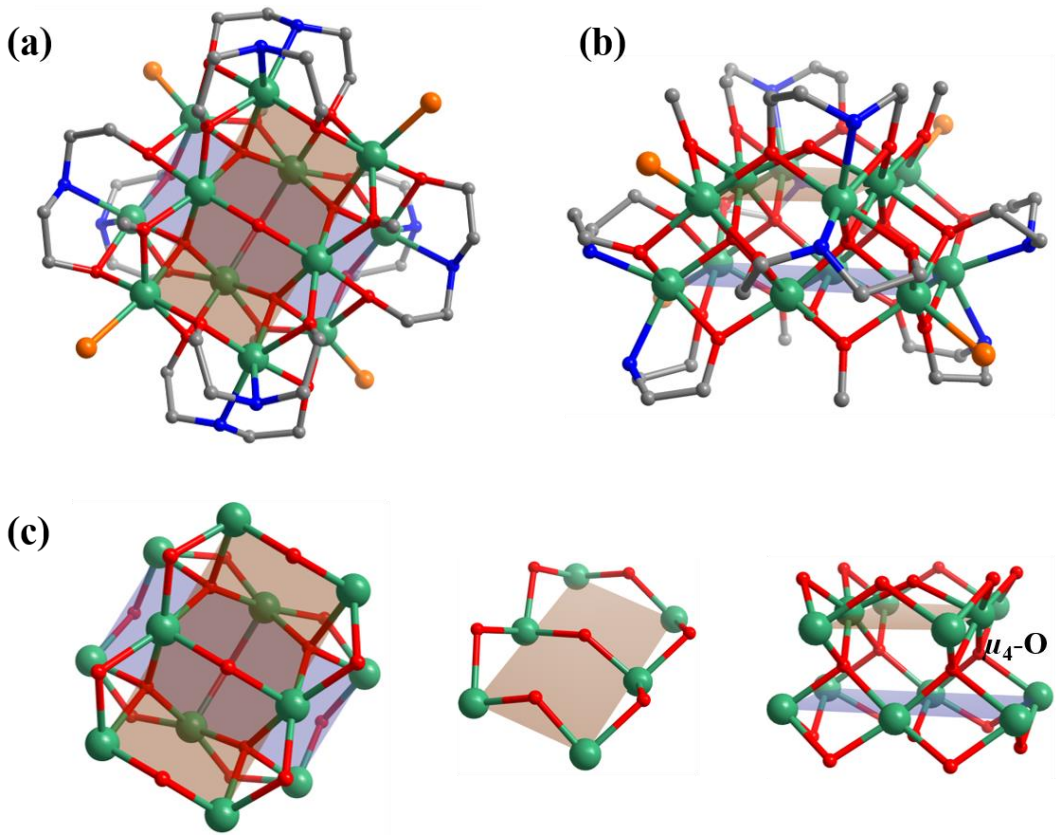

Figure S2 Top view **(a)** and side view **(b)** towards molecular structure of **InOC-1** with highlighted In_6 building units. **(c)** Illustration of the rectangular In_6 building units and the arrangements of two pairs of In_6-rectangle in **InOC-1** to **InOC-5**.

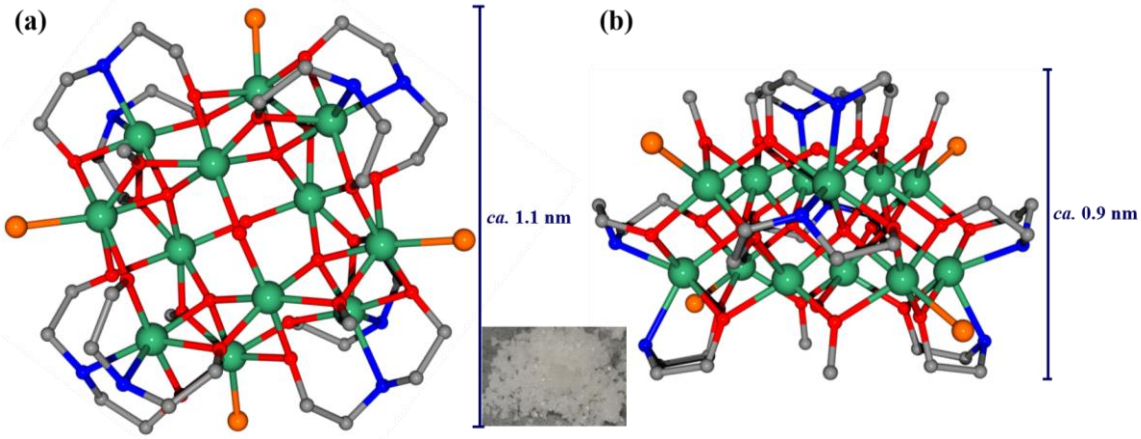

Figure S3 Molecular structure of **InOC-1** in top view **(a)** and side view **(b)**. The side length and thickness are also presented.

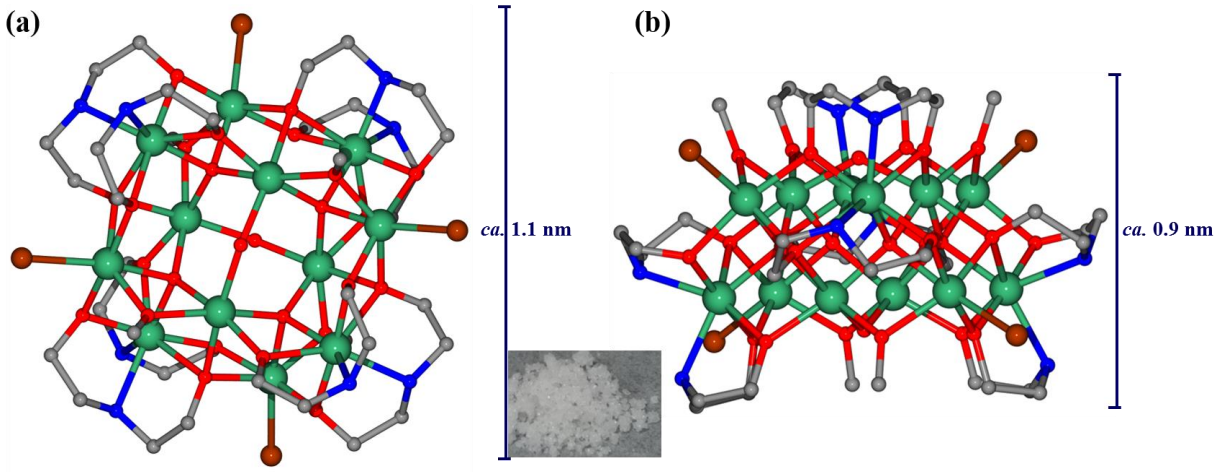

Figure S4 Molecular structure of **InOC-2** in top view **(a)** and side view **(b)**. The side length and thickness are also presented.

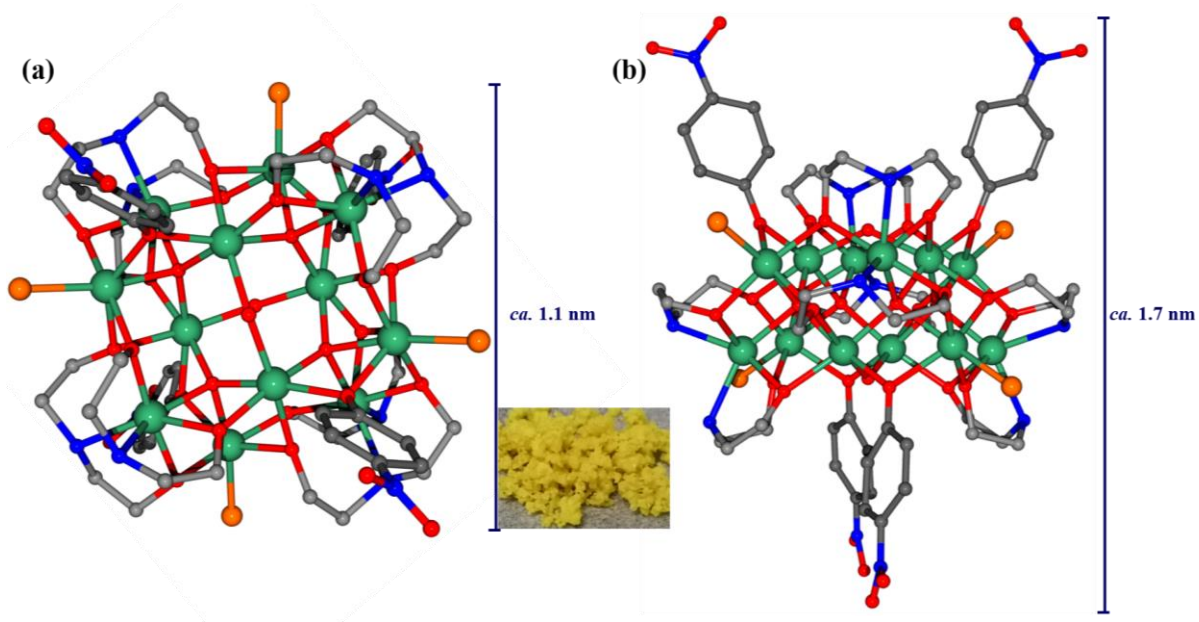

Figure S5 Molecular structure of **InOC-3** in top view **(a)** and side view **(b)**. The side length and thickness are also presented.

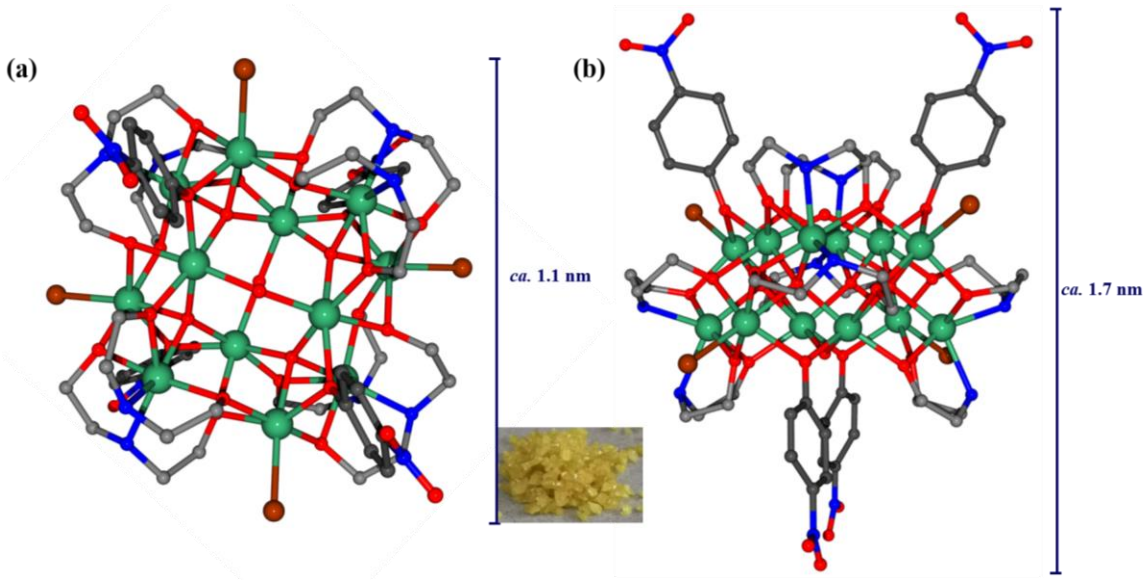

Figure S6 Molecular structure of **InOC-4** in top view **(a)** and side view **(b)**. The side length and thickness are also presented.

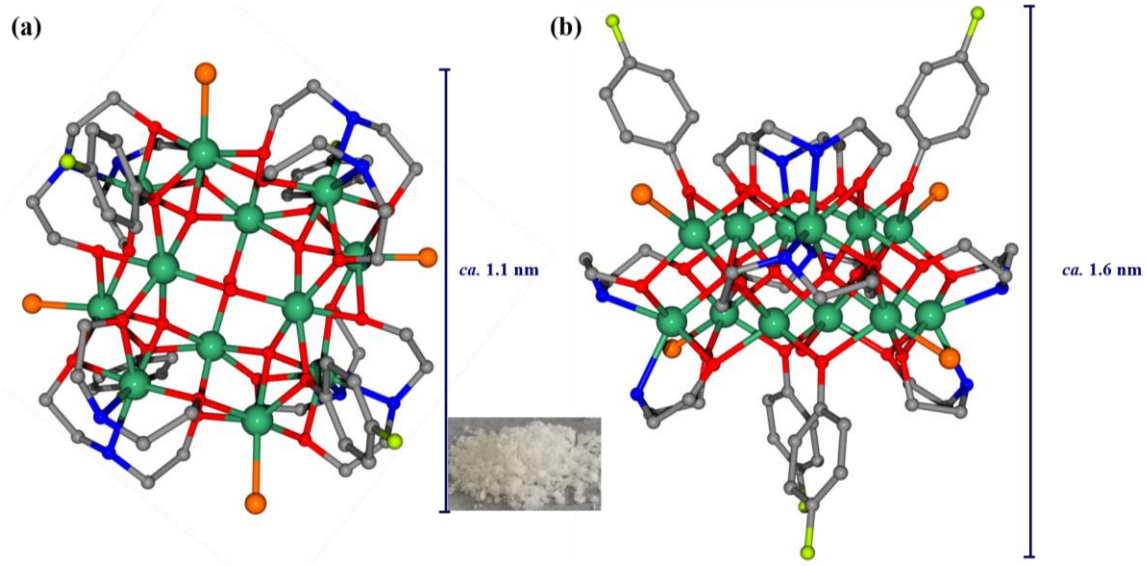

Figure S7 Molecular structure of **InOC-5** in top view **(a)** and side view **(b)**. The side length and thickness are also presented.

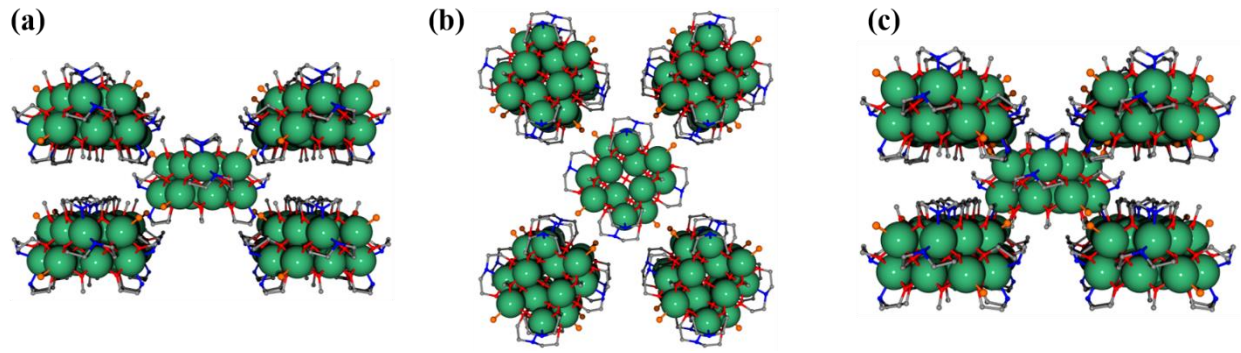

Figure S8 Packing mode of **InOC-1** along axis *a*, *b* and *c*.

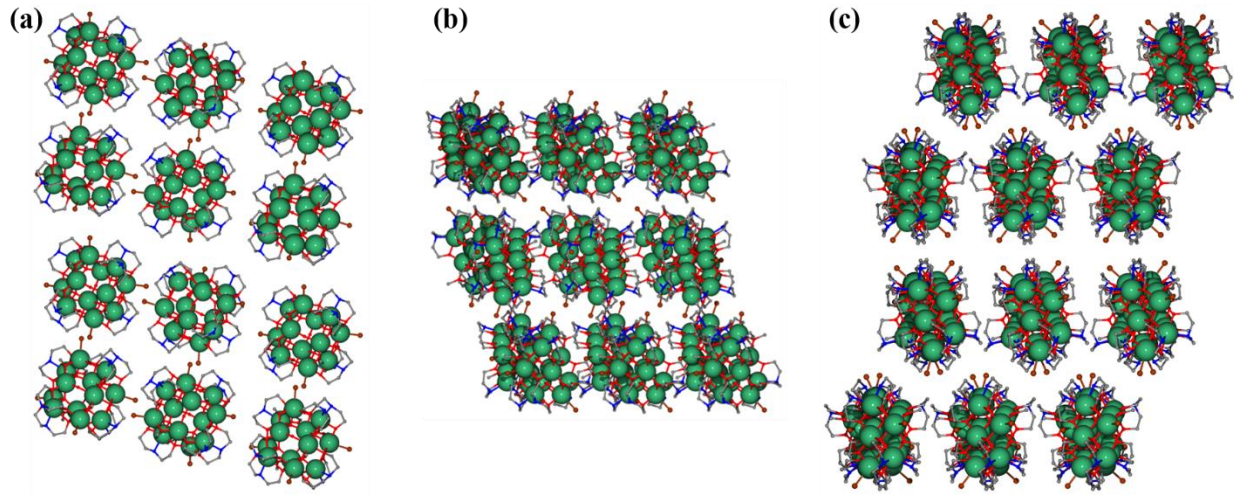

Figure S9 Packing mode of **InOC-2** along axis *a*, *b* and *c*.

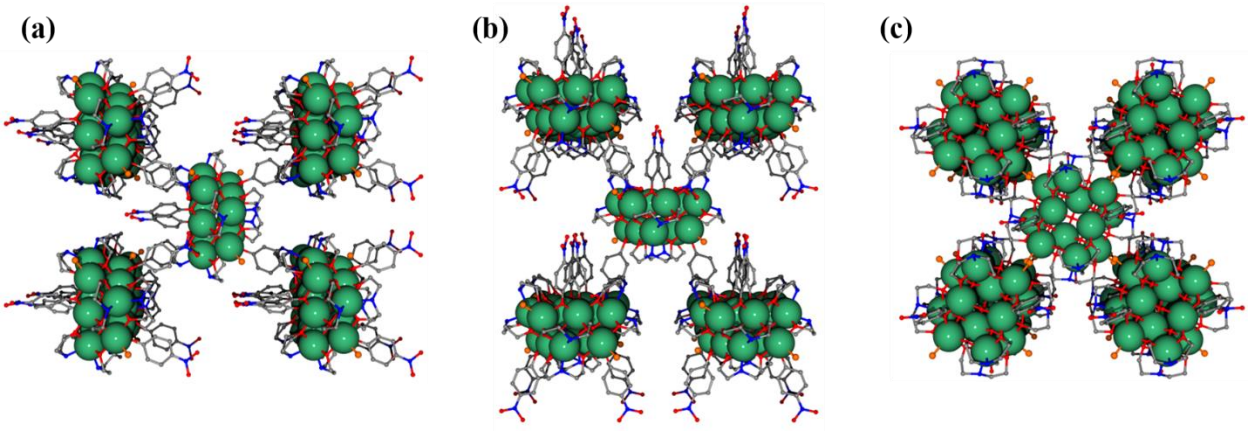

Figure S10 Packing mode of **InOC-3** along axis *a*, *b* and *c*.

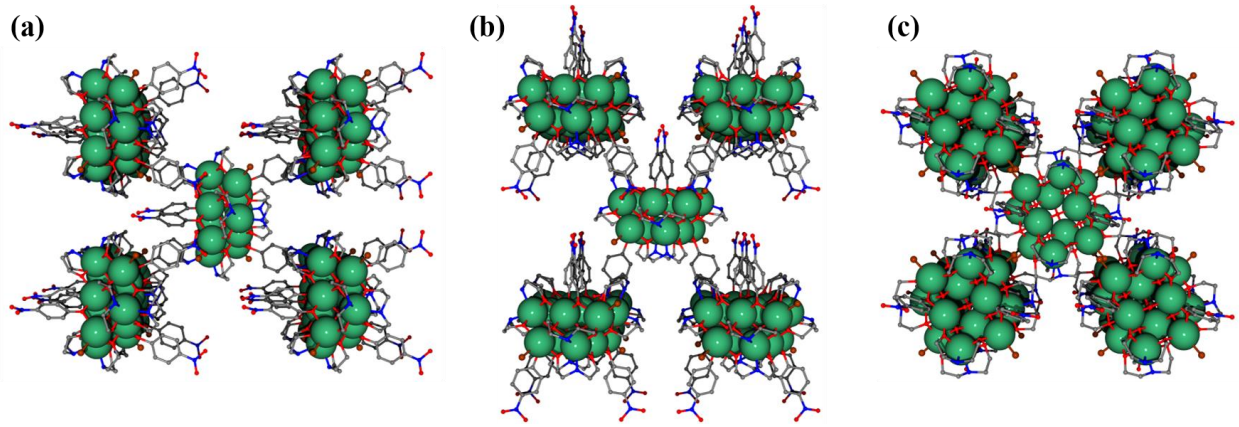

Figure S11 Packing mode of **InOC-4** along axis *a*, *b* and *c*.

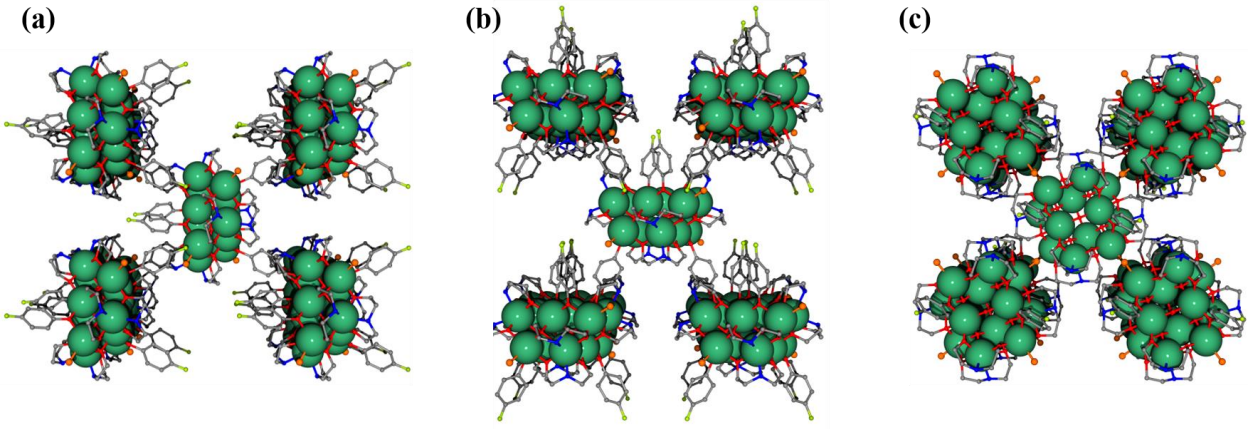

Figure S12 Packing mode of **InOC-5** along axis *a*, *b* and *c*.

VI. Powder-XRD patterns

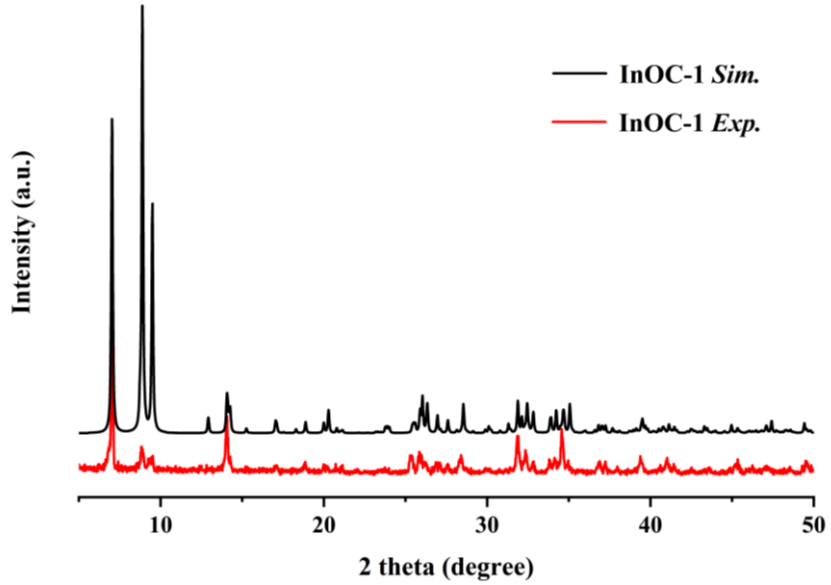

Figure S13 P-XRD analysis for **InOC-1**.

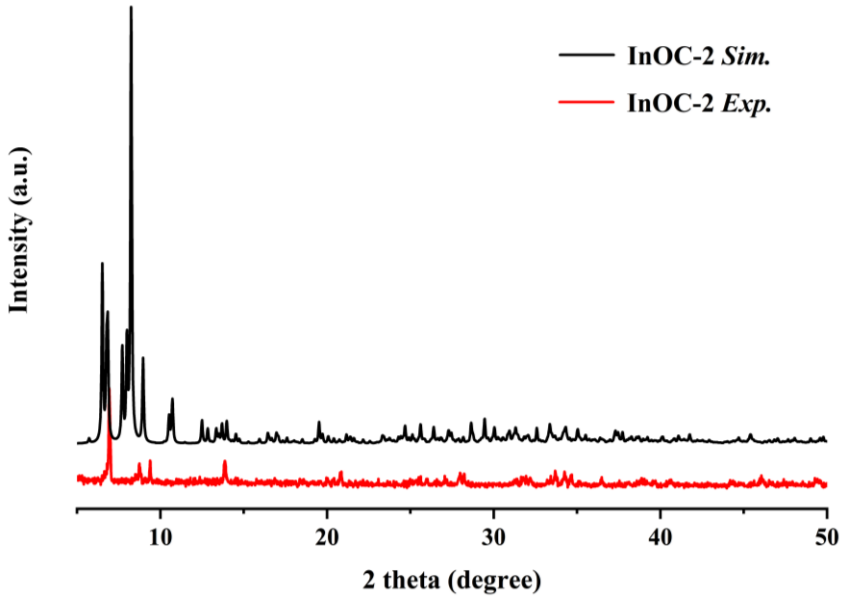

Figure S14 P-XRD analysis for **InOC-2**.

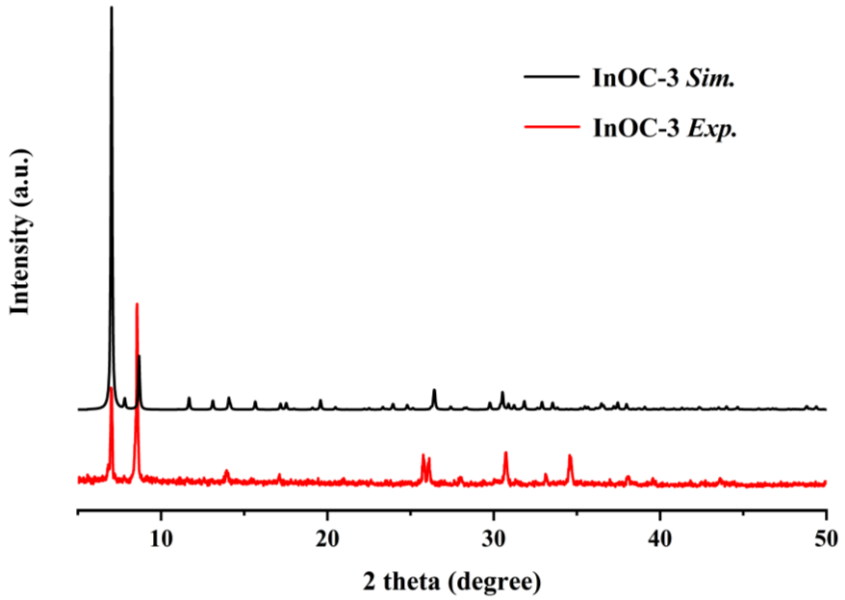

Figure S15 P-XRD analysis for **InOC-3**.

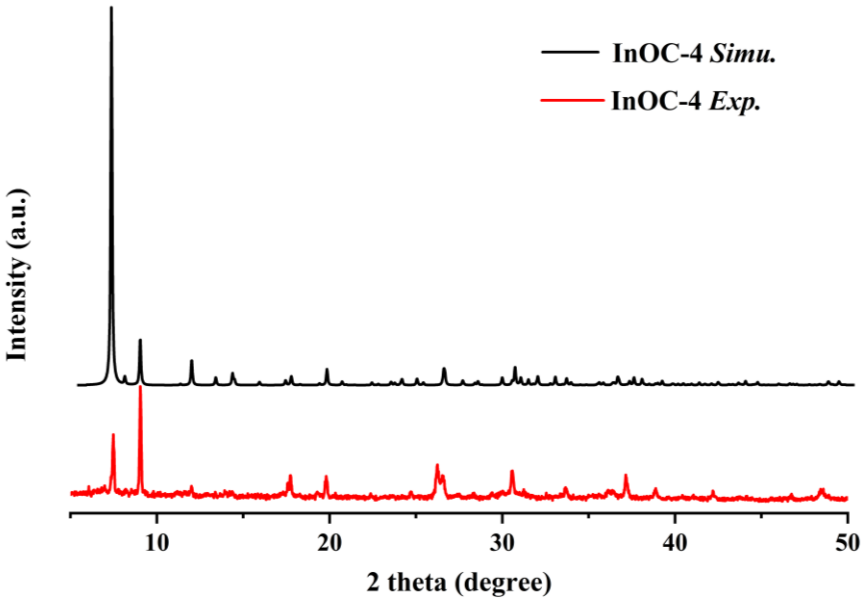

Figure S16 P-XRD analysis for **InOC-4**.

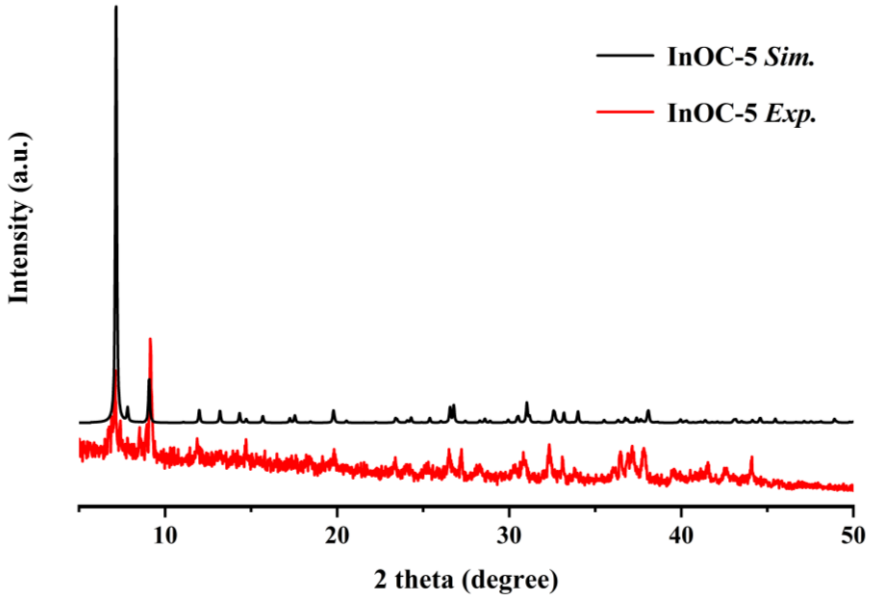

Figure S17 P-XRD analysis for **InOC-5**.

VII. The energy dispersive X-ray spectroscopy (EDS) spectra

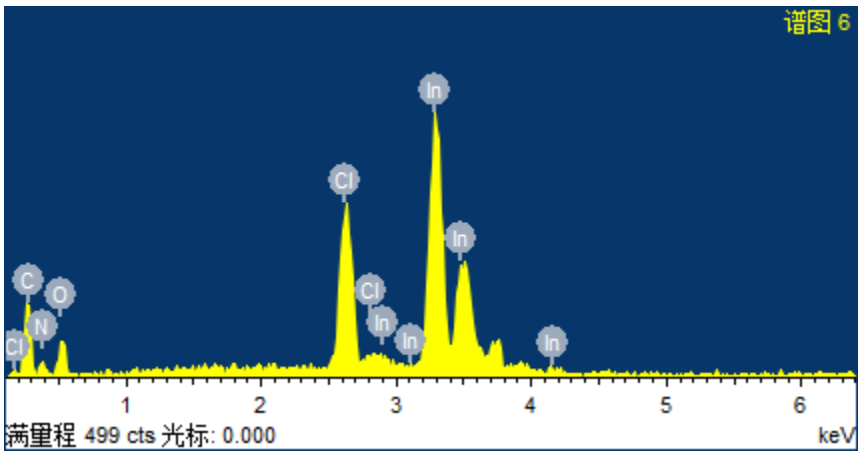

Figure S18 The EDS spectrum of **InOC-1**

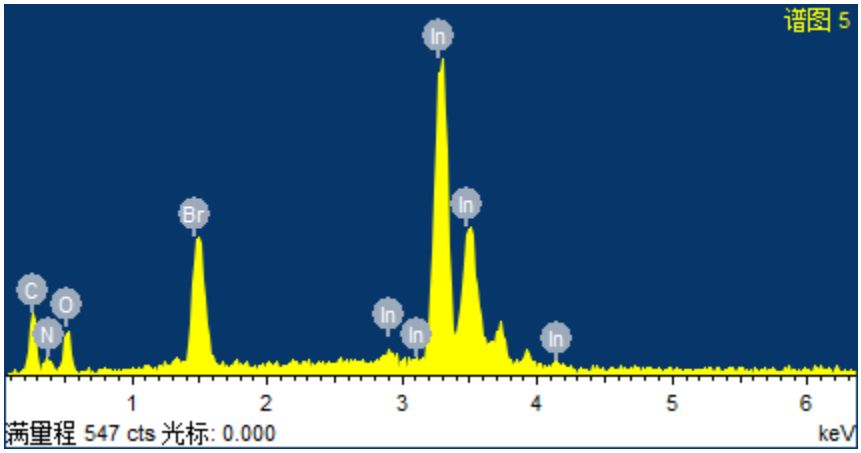

Figure S19 The EDS spectrum of **InOC-2**

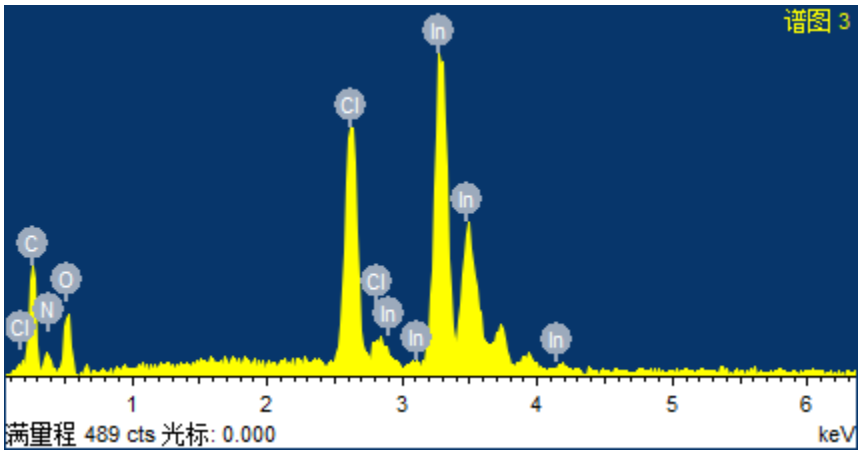

Figure S20 The EDS spectrum of **InOC-3**

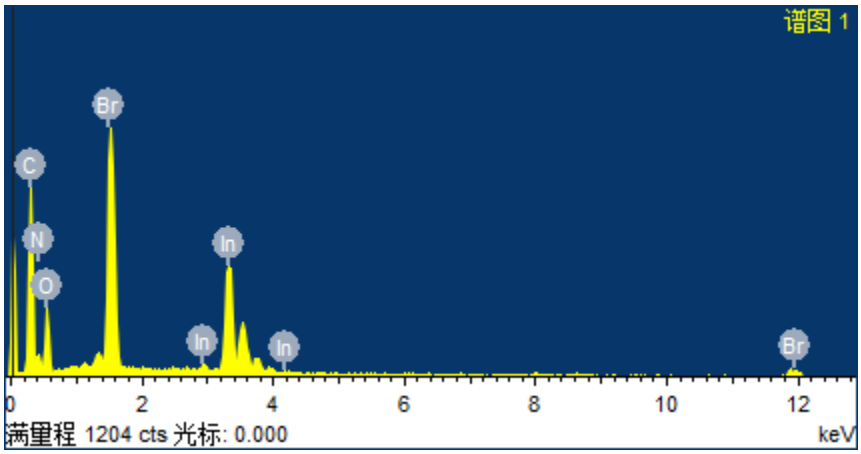

Figure S21 The EDS spectrum of **InOC-4**

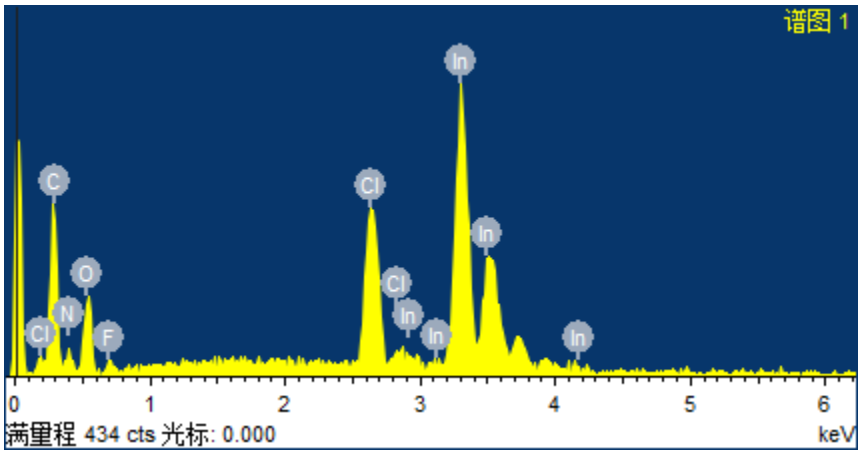

Figure S22 The EDS spectrum of **InOC-5**

VIII. Thermogravimetrical analysis (TGA)

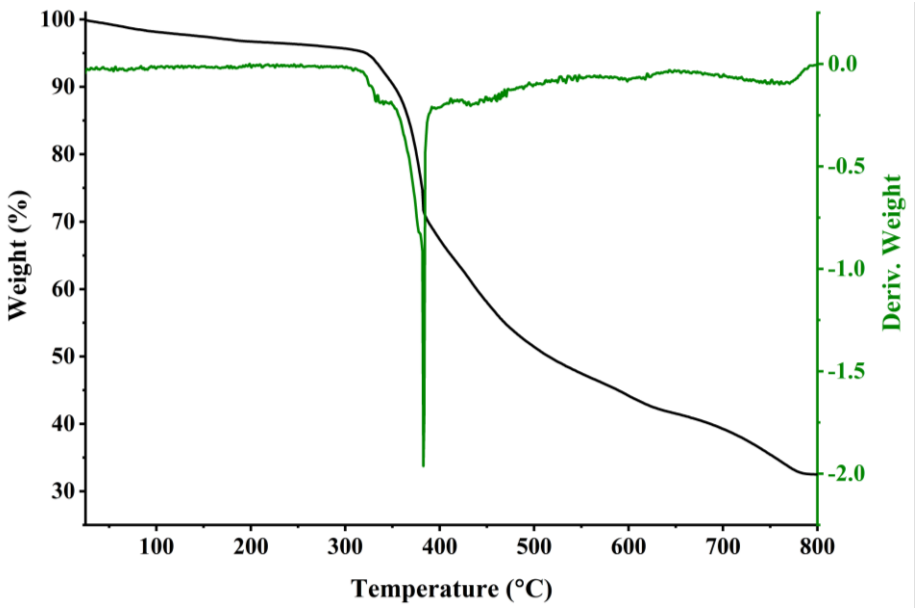

Figure S23 TGA (black), derivative TGA (green) and curves for **InOC-1** from room temperature to 800 °C under N_2 atmosphere.

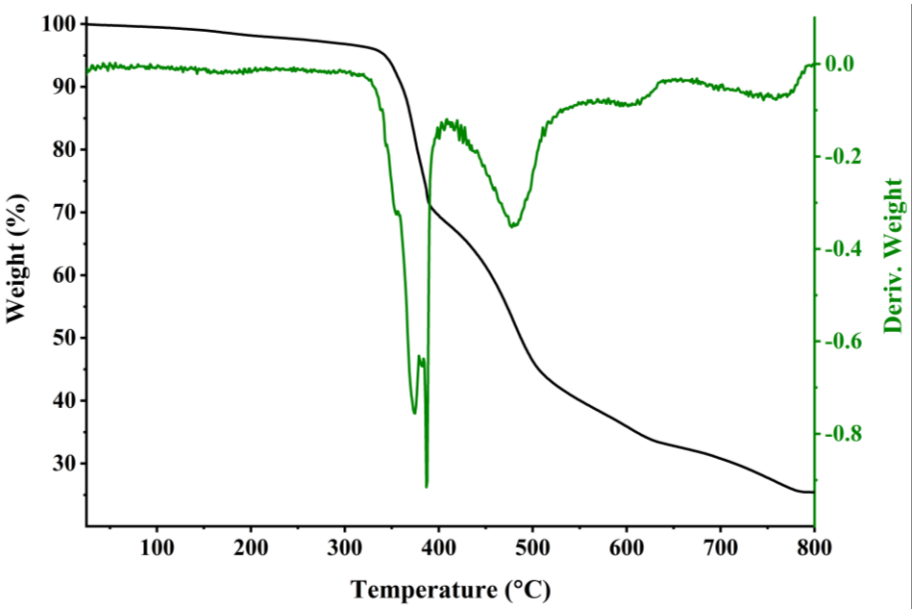

Figure S24 TGA (black), derivative TGA (green) and curves for **InOC-2** from room temperature to 800 °C under N_2 atmosphere.

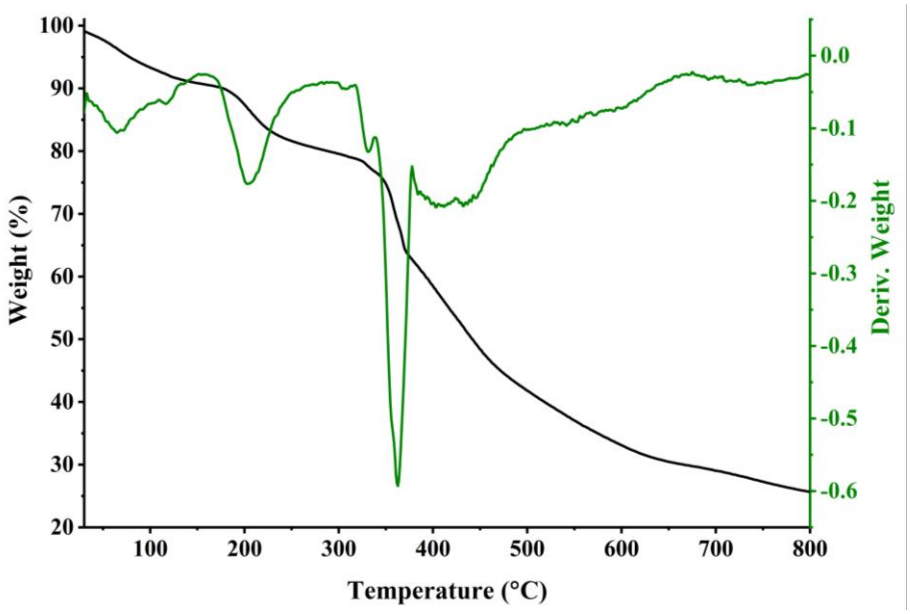

Figure S25 TGA (black), derivative TGA (green) and curves for **InOC-3** from room temperature to 800 °C under N_2 atmosphere.

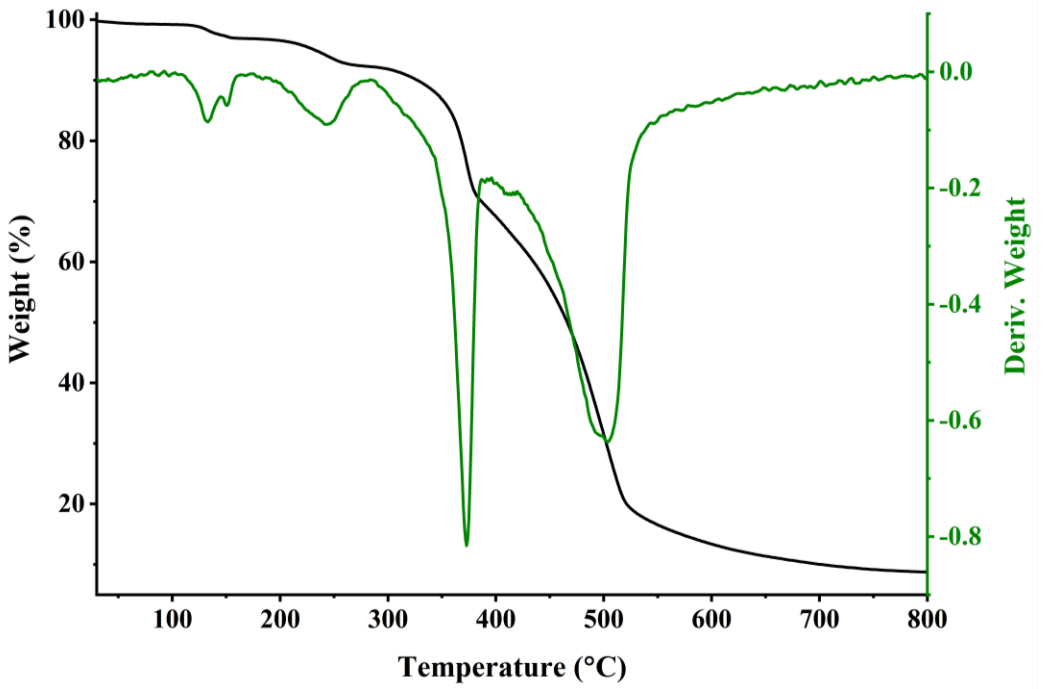

Figure S26 TGA (black), derivative TGA (green) and curves for **InOC-4** from room temperature to 800 °C under N_2 atmosphere.

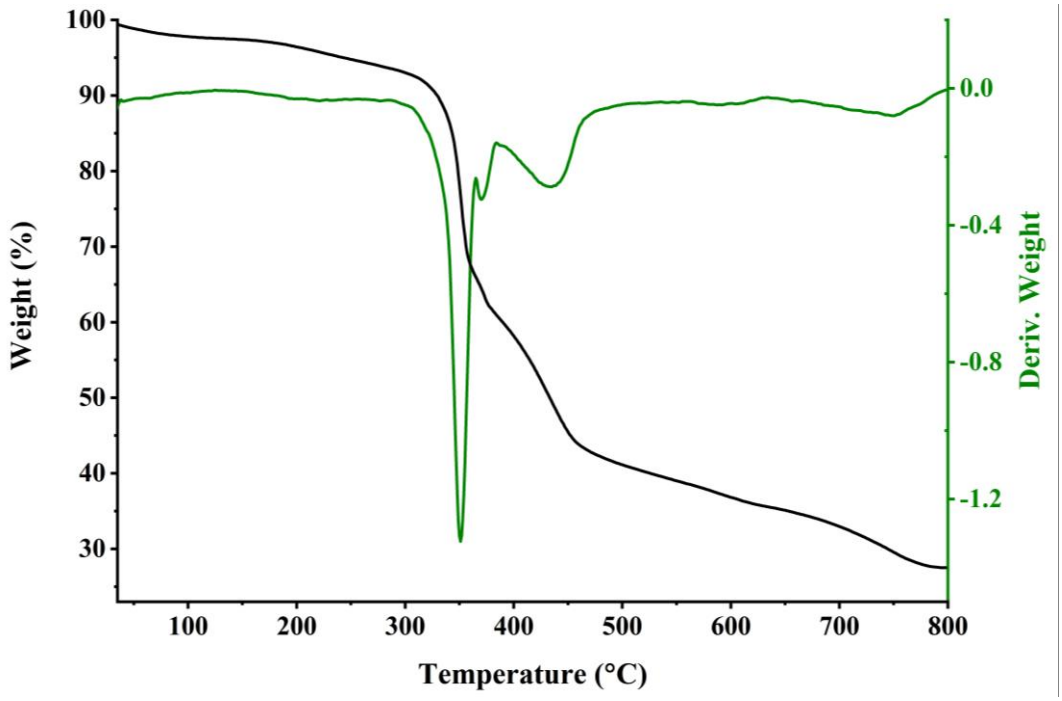

Figure S27 TGA (black), derivative TGA (green) and curves for **InOC-5** from room temperature to 800 °C under N_2 atmosphere.

IX. IR spectra

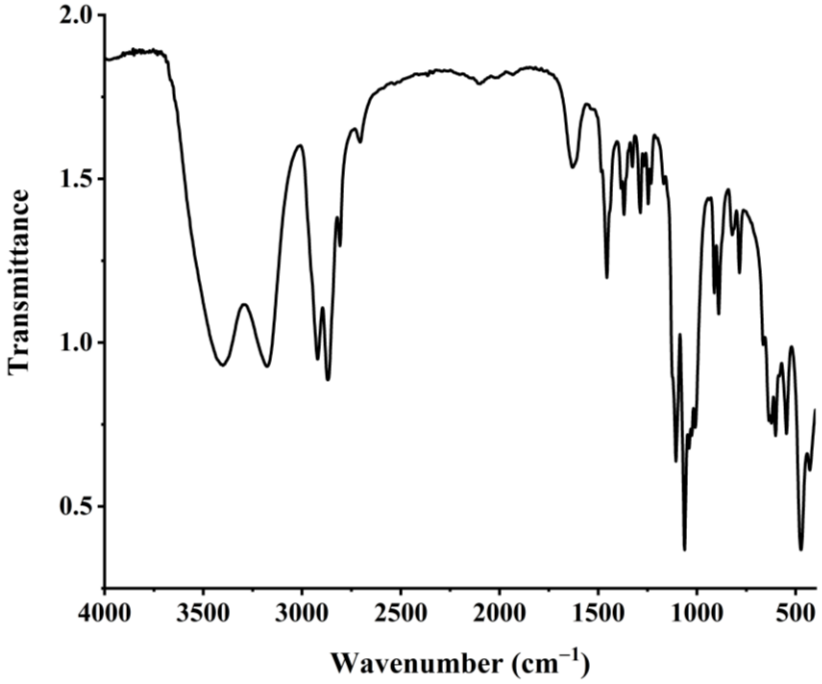

Figure S28 FT-IR spectrum of **InOC-1**.

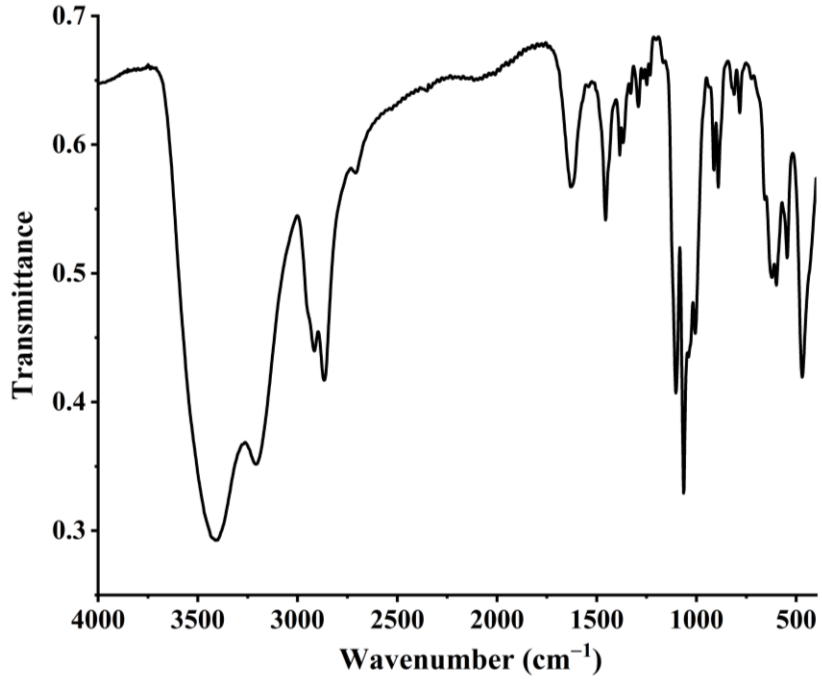

Figure S29 FT-IR spectrum of **InOC-2**.

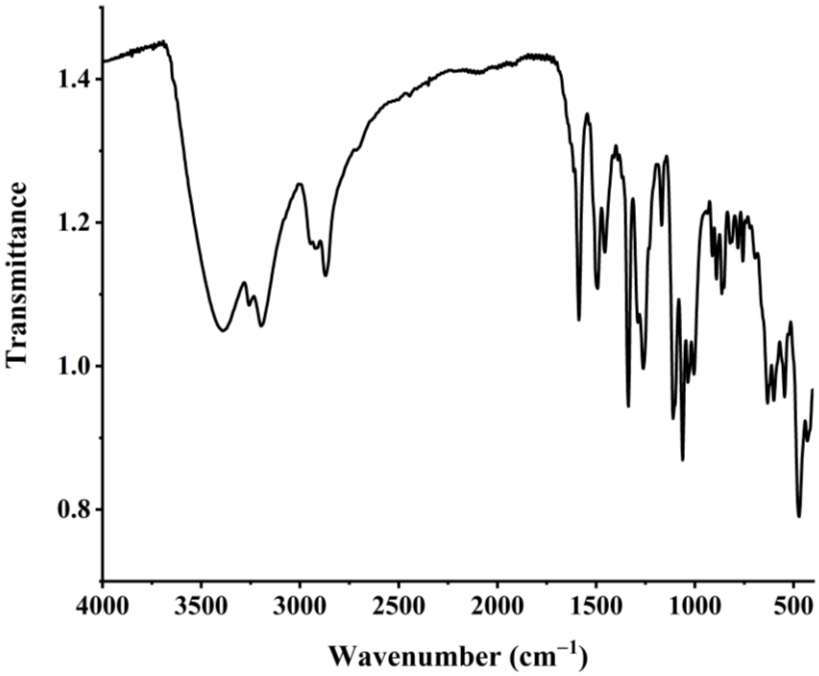

Figure S30 FT-IR spectrum of **InOC-3**.

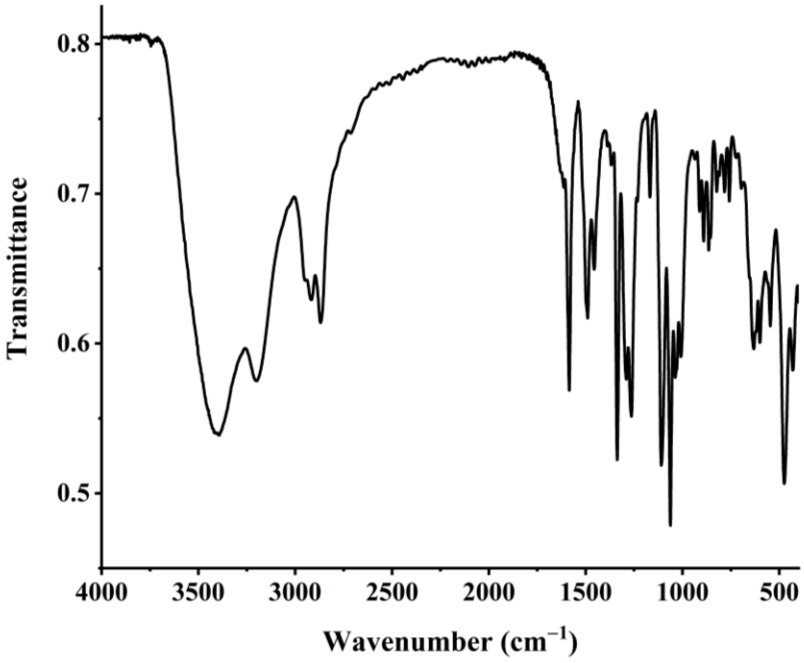

Figure S31 FT-IR spectrum of **InOC-4**.

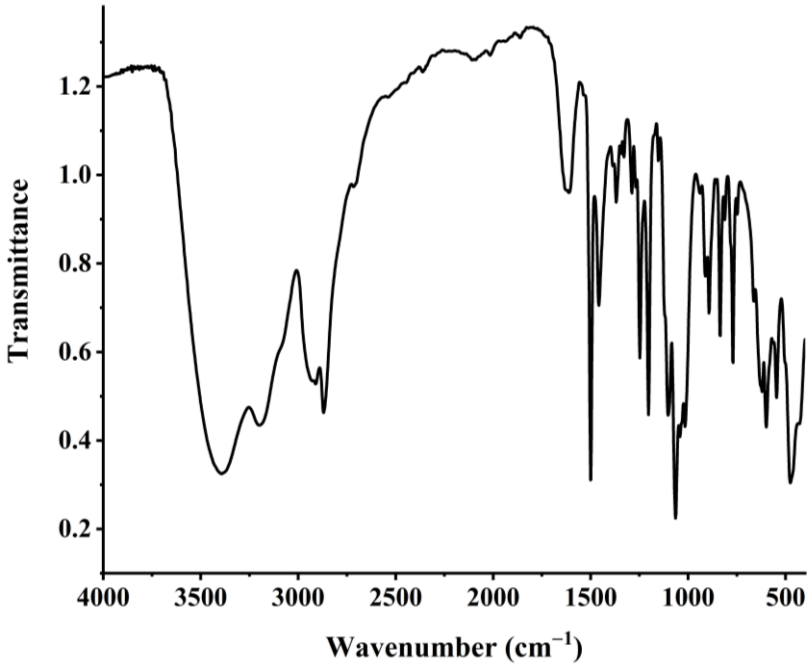

Figure S32 FT-IR spectrum of **InOC-5**.

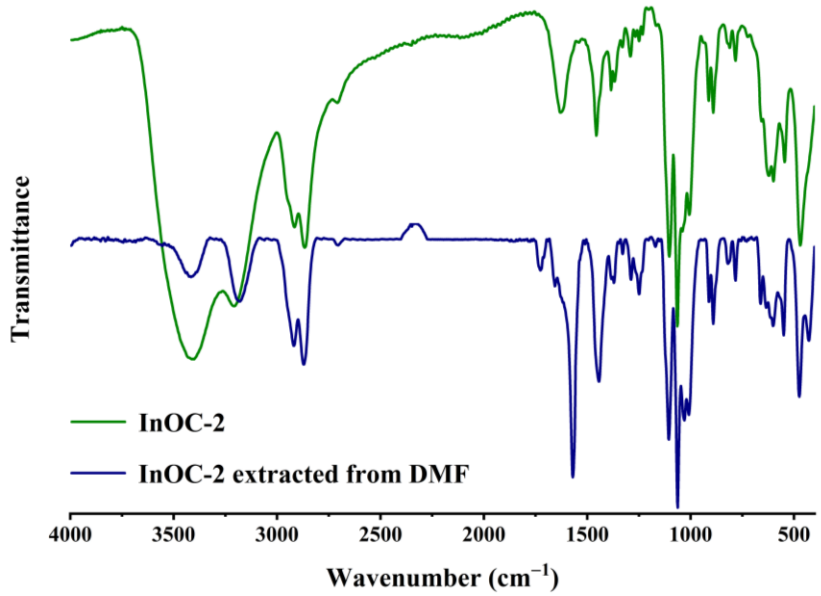

Figure S33 Comparison of FT-IR spectra of **InOC-2** (olive) and **InOC-2** dissolved in DMF followed by extraction with assistance of PGMEA (navy).

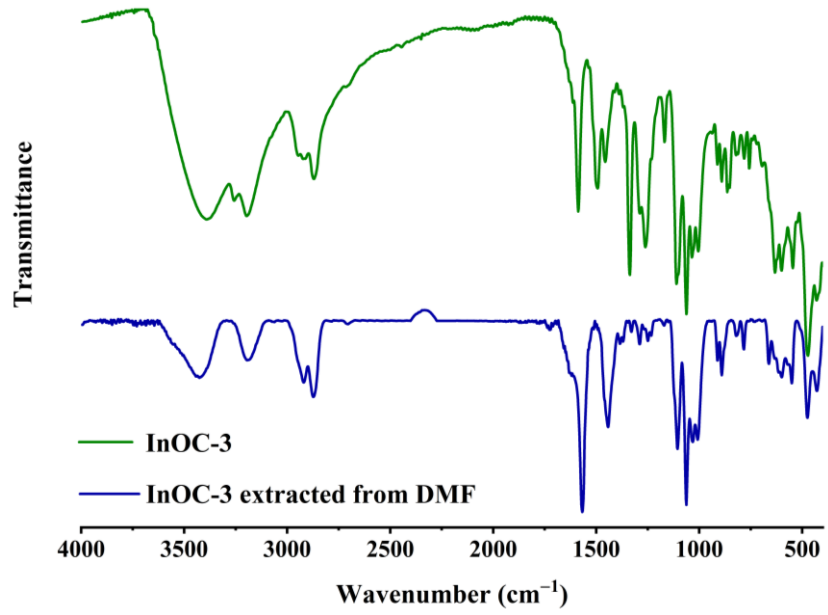

Figure S34 Comparison of FT-IR spectra of **InOC-3** (olive) and **InOC-3** dissolved in DMF followed by extraction with assistance of PGMEA (navy).

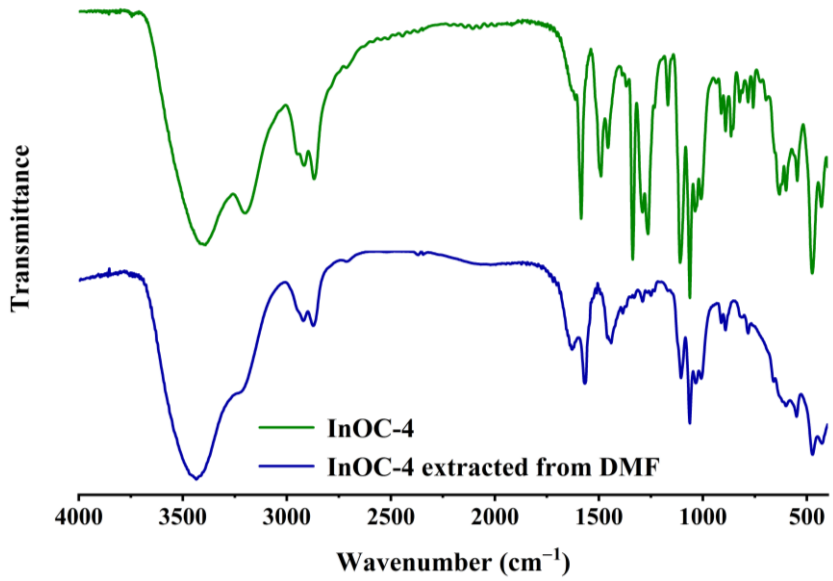

Figure S35 Comparison of FT-IR spectra of **InOC-4** (olive) and **InOC-4** dissolved in DMF followed by extraction with assistance of PGMEA (navy).

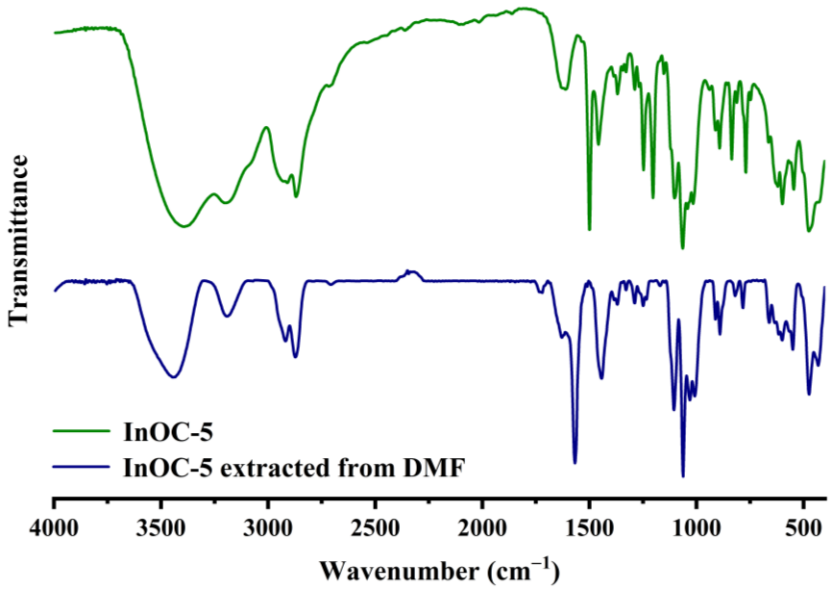

Figure S36 Comparison of FT-IR spectra of **InOC-5** (olive) and **InOC-5** dissolved in DMF followed by extraction with assistance of PGMEA (navy).

X. Electrospray ionization mass spectrometry measurements (ESI-MS)

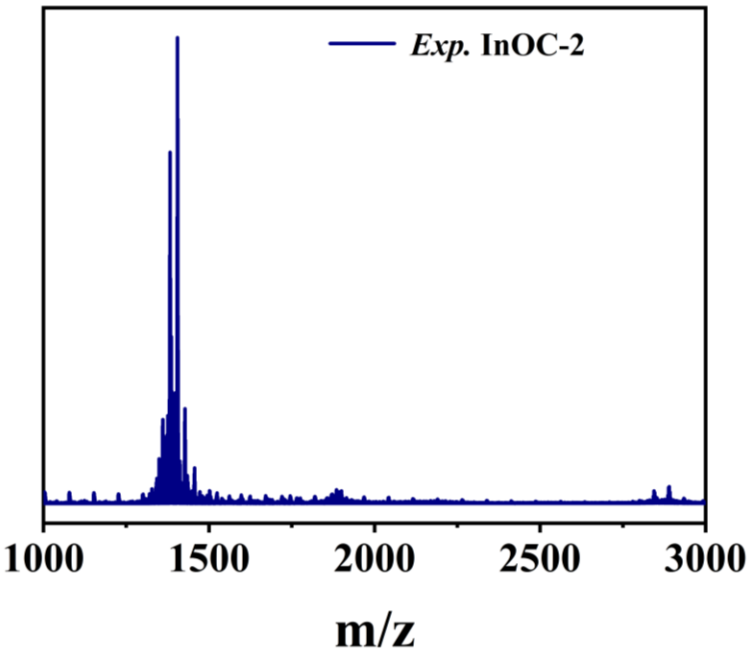

Figure S37 Positive-mode ESI-MS spectrum of the mother liquor of **InOC-2**.

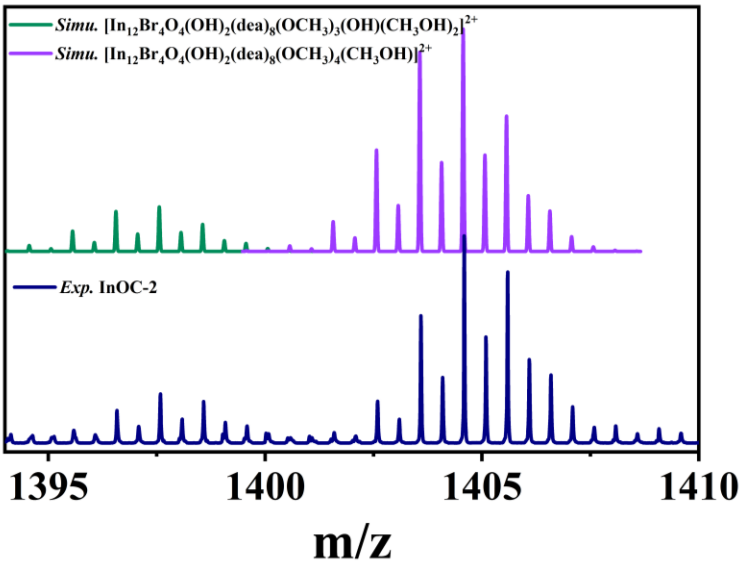

Figure S38 The comparison of experimental isotopic envelop with simulated patterns of the predominant species of +2 charged $\{In_{12}\text{-cluster}\}^{2+}$ **InOC-2**.

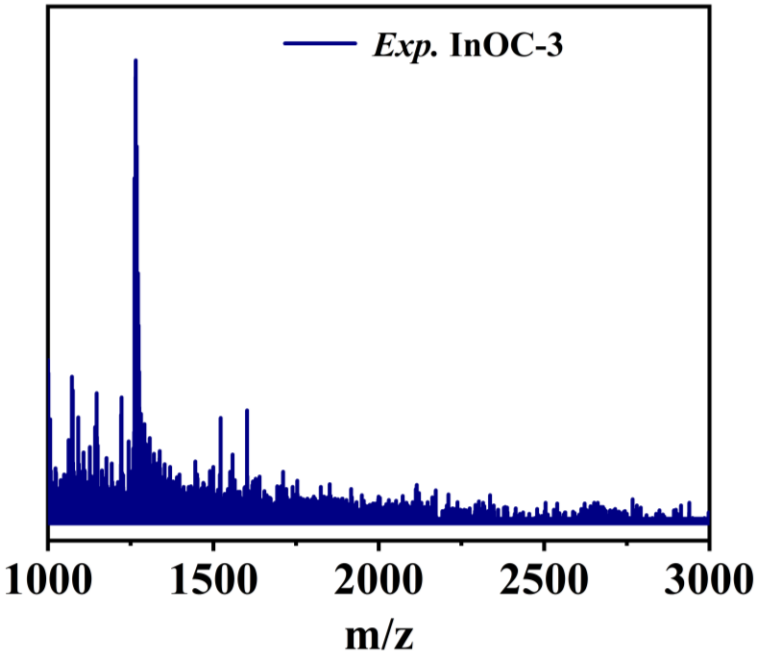

Figure S39 Positive-mode ESI-MS spectrum of **InOC-3** in DMF.

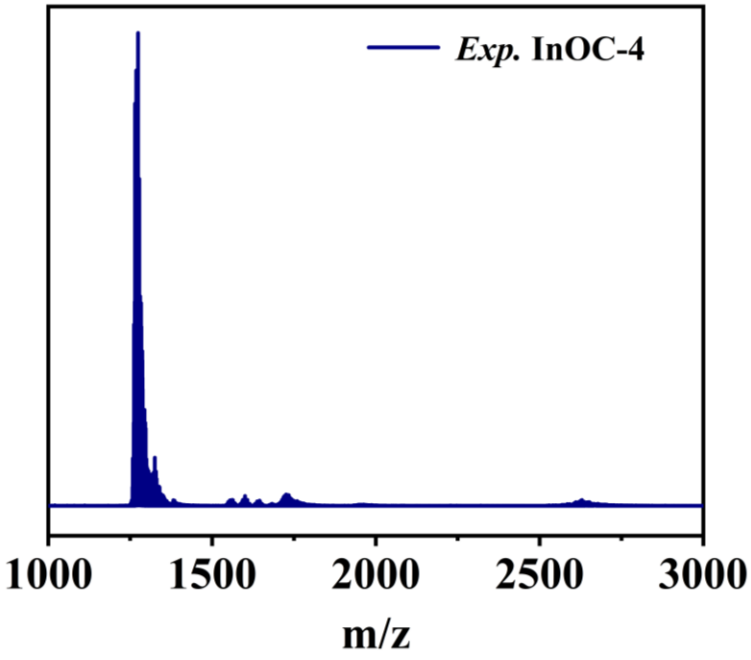

Figure S40 Positive-mode ESI-MS spectrum of **InOC-4** in DMF.

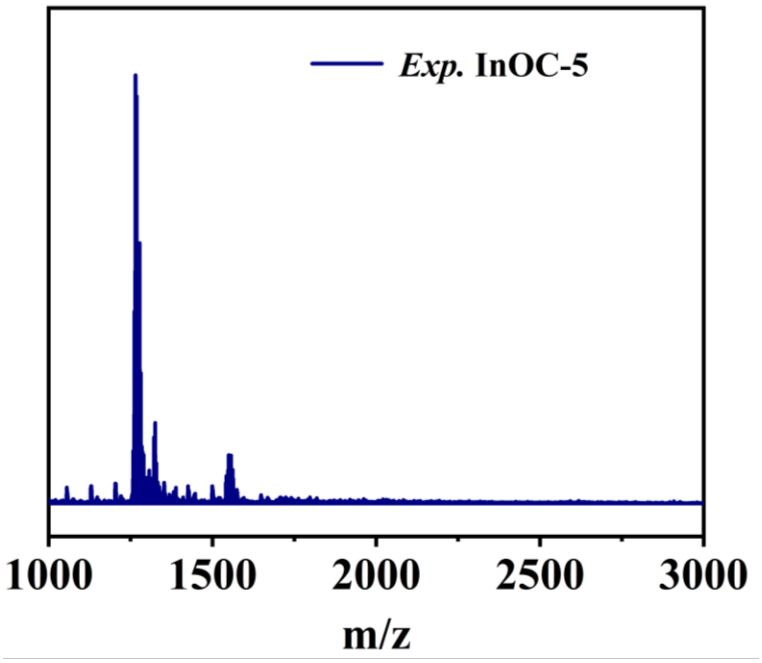

Figure S41 Positive-mode ESI-MS spectrum of **InOC-5** in DMF.

Table S11 Peak assignments for positive mode ESI-MS of **InOC-1** in DMF.

Envelop assignment	charge	m/z (*exp.*)	m/z (*cal.*)
$[In_{12}Cl_4O_4(OH)_2(OCH_2CH_2NHCH_2CH_2O)_8(OH)_4]^{2+}$	+2	1254.57	1254.61
$[In_{12}Cl_3O_4(OH)_2(OCH_2CH_2NHCH_2CH_2O)_8(OCH_3)_3(OH)]^{2+}$	+2	1258.09	1258.15
$[In_{12}Cl_4O_4(OH)_2(OCH_2CH_2NHCH_2CH_2O)_8(OCH_3)(OH)_3]^{2+}$	+2	1261.59	1261.61
$[In_{12}Cl_3O_4(OH)_2(OCH_2CH_2NHCH_2CH_2O)_8(OCH_3)_4]^{2+}$	+2	1265.09	1265.18
$[In_{12}Cl_4O_4(OH)_2(OCH_2CH_2NHCH_2CH_2O)_8(OCH_3)_2(OH)_2]^{2+}$	+2	1268.51	1268.62

Table S12 Peak assignments for positive mode ESI-MS of **InOC-2** mother liquor.

Envelop assignment	charge	m/z (*exp.*)	m/z (*cal.*)
$[In_{12}Br_4O_4(OH)_2(OCH_2CH_2NHCH_2CH_2O)_8(OCH_3)_4(CH_3OH)_2]^{2+}$	+2	1402.60	1402.57
$[In_{12}Br_4O_4(OH)_2(OCH_2CH_2NHCH_2CH_2O)_8(OCH_3)_3(OH)(CH_3OH)_2]^{2+}$	+2	1395.56	1395.56

XI. UV-Vis parameters

Table S13 The concentration of the materials during the UV-Vis experiments.

Code	Concentration (mol/L)	Code	Concentration (mol/L)
InOC-3	$5.92*10^{-5}$	**InOC-4**	$6.112*10^{-5}$
InOC-5	$1.16*10^{-4}$	***p*-Nitrophenol**	$1.02*10^{-3}$
***p*-Flurophenol**	$2.86*10^{-3}$		

XII. Patterning performance investigations

The 12~14 mg/mL DMF solution of **InOC-1**, **InOC-2** and **InOC-3** was spin-coated onto a pre-clean silicon wafer at 2000 or 3000 rpm for 30 seconds followed by baking on a hot plate at 70 °C for 30 seconds. The film with a thickness of ca. 14 to 20 nm was then exposed to electron beam radiation with doses of 10 to 1200 μC/cm^2. As indicated in the scanning electron microscope (SEM) and atomic force microscope (AFM) images, well-defined negative tone patterns were obtained after development. Unfortunately, no matter on the hydrophilic or hydrophobic Si-substrate, **InOC-4** or **InOC-5** only formulated poor quality films unsuitable for EBL evaluations. We think the subtle fluctuations in the structures or compositions of the In_{12}-oxo clusters dominate their Hansen solubility parameters (HSP) and surface tension of the resulting solution, which determine whether smooth films can be formed on the Si-substrate.

Table S14 Film thickness of **InOC-1** to **InOC-3** on the Si-wafer.

Code	Thickness (nm)	Code	Thickness (nm)	Code	Thickness (nm)
InOC-1	15	**InOC-2**	18	**InOC-3**	14

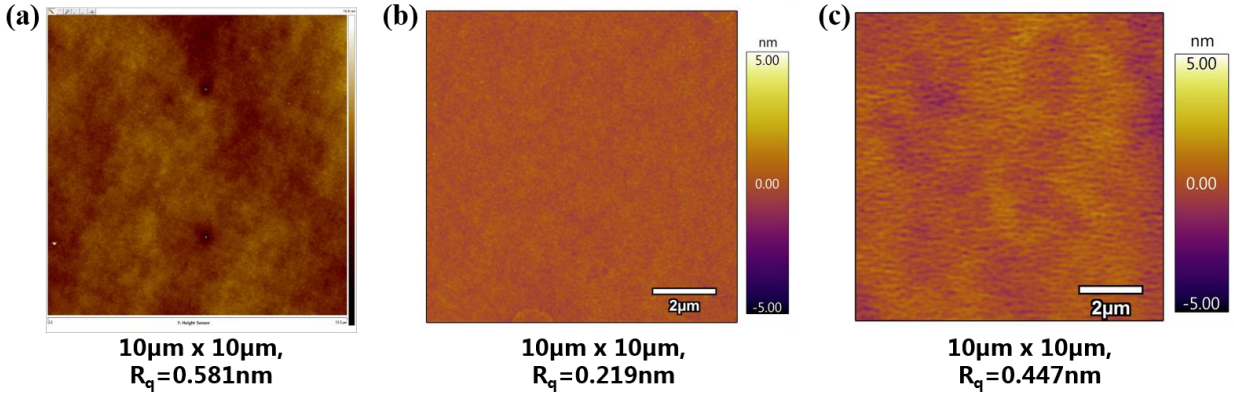

Figure S42 Topographic AFM images with Rq roughness in the areas of 10μm x 10μm for **InOC-1 (a)**, **InOC-2 (b)**, **InOC-3 (c)**. R_q roughness is defined here as the square root of the arithmetic mean of the squares of each z value measured on an AFM image.

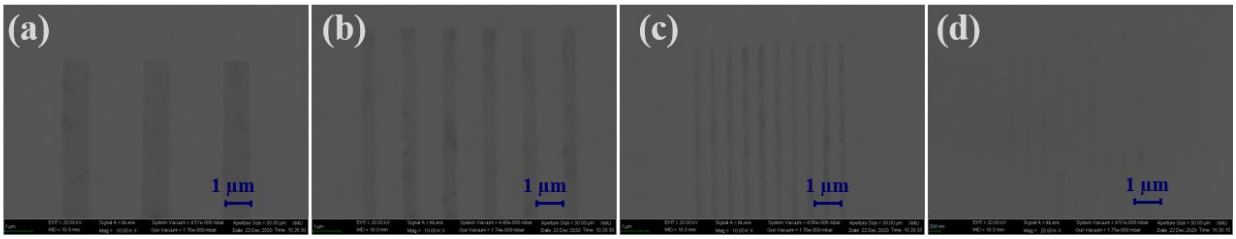

Figure S43 SEM images of patterns performed with dose of 1000 μC/cm^2 exhibiting different feature sizes of 1 µm **(a)**, 500 nm **(b)**, 200 nm **(c)** and 100 nm **(d)** for **InOC-1**.

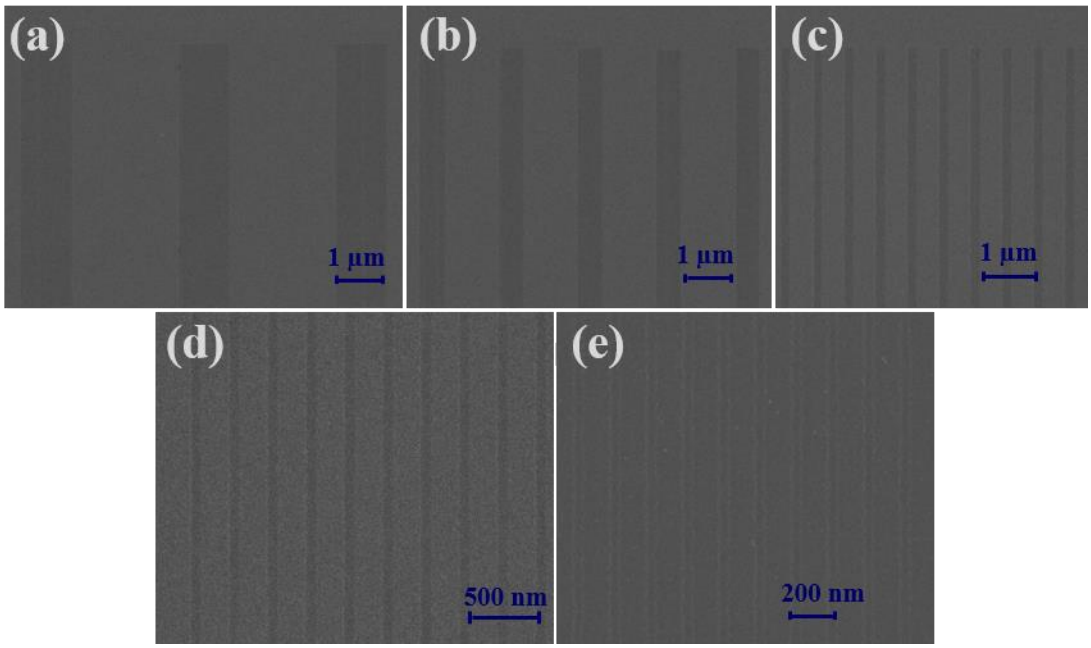

Figure S44 SEM images of patterns performed with dose of 1000 μC/cm^2 exhibiting different feature sizes of 1 µm **(a)**, 500 nm **(b)**, 200 nm **(c)**, 100 nm **(d)** and 50 nm **(e)** for **InOC-2**.

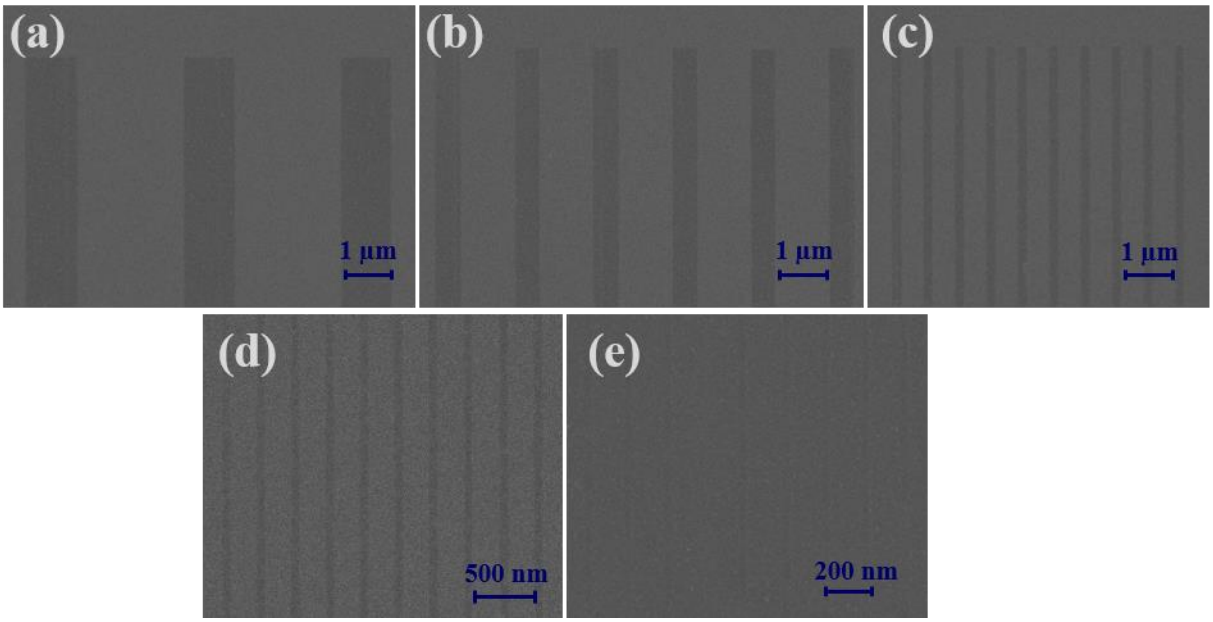

Figure S45 SEM images of patterns performed with dose of 1000 μC/cm^2 exhibiting different feature sizes of 1 µm **(a)**, 500 nm **(b)**, 200 nm **(c)**, 100 nm **(d)** and 50 nm **(e)** for **InOC-3**.

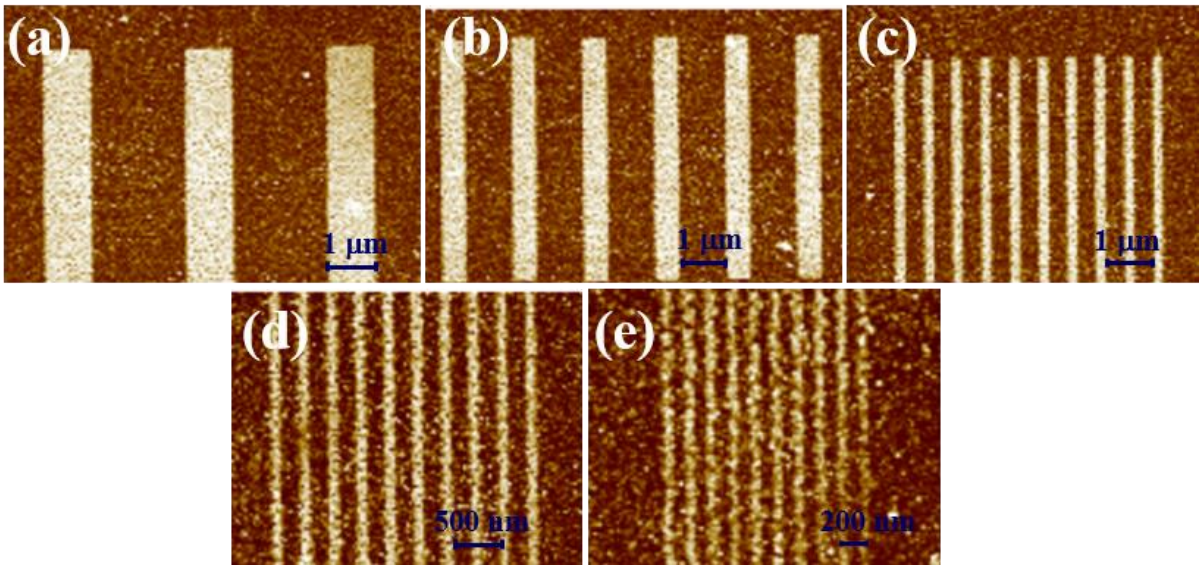

Figure S46 AFM images of patterns performed with dose of 500 μC/cm^2 exhibiting different feature sizes of 1 µm **(a)**, 500 nm **(b)**, 200 nm **(c)**, 100 nm **(d)** and 50 nm **(e)** for **InOC-3**.

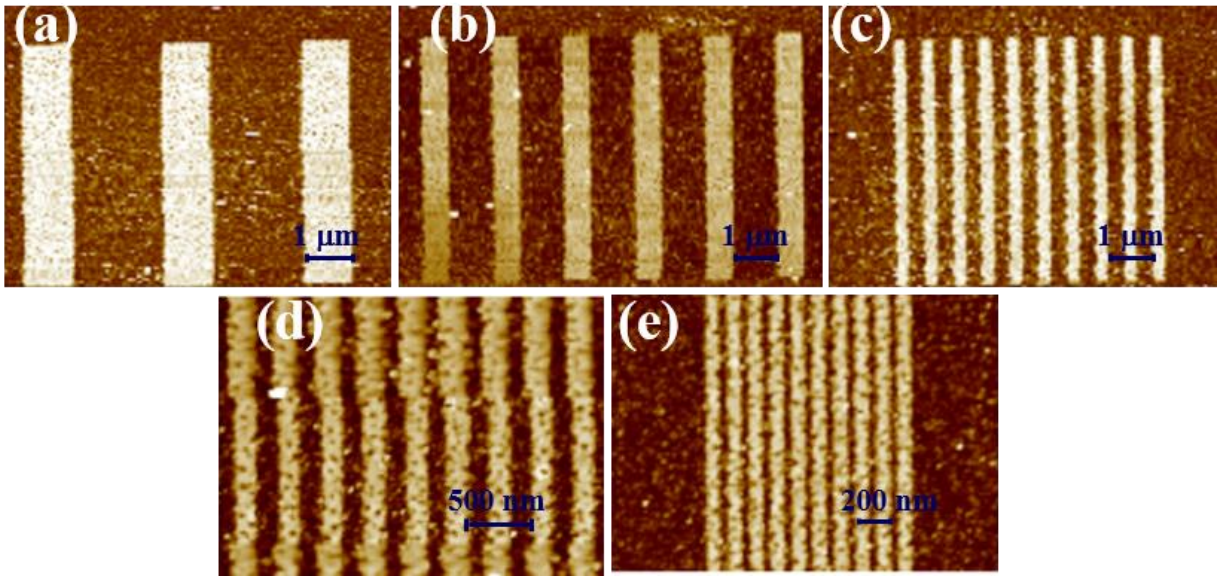

Figure S47 AFM images of patterns performed with dose of 1000 μC/cm^2 exhibiting different feature sizes of 1 µm **(a)**, 500 nm **(b)**, 200 nm **(c)**, 100 nm **(d)** and 50 nm **(e)** for **InOC-3**.

[1] O. V. Dolomanov, L. J. Bourhis, R. J. Gildea, J. A. K. Howard, H. Puschmann, *J. Appl. Crystallogr.* **2009**, *42*, 339-341.

[2] a) G. M. Sheldrick, *Acta Crystallogr.* **2015**, *C71*, 3-8; b) G. M. Sheldrick, *Acta Crystallogr.* **2008**, *A64*, 112-122.

[3] a) I. D. Brown, D. Altermatt, *Acta Crystallogr.* **1985**, *B41*, 244-247; b) K. Knížek, *Kalvados – Software for crystal structure and powder diffraction; see http://www.fzu.cz/~knizek/kalvados/index.html*.